ORIGINAL PAPER - EXPLORATION GEOPHYSICS

Investigation of reservoir characteristics, depositional setting and T–R sequences of the Lockhart Limestone of Meyal Oil Field, Pakistan: a petrophysical approach

Muhammad Awais[1] · Farhad Ullah[1] · Nasar Khan[2] · Mukhtiar Ghani[3] · Syed Mamoon Siyar[2] · Bilal Wadood[1] · Aizaz Mukhtiar[1]

Abstract

The present study is focused on formation evaluation of the Lockhart Limestone in two wells (Meyal-05P and Meyal-10P) located in Northern Deformed Potwar Zone of the Potwar sub-basin, Pakistan. The geological formations ranging from Triassic to Pliocene have been drilled in these wells. The formation evaluation of the Lockhart Limestone mainly involves reservoir potential evaluation, interpretation of depositional environment and transgressive–regressive sequences using petrophysical logs. In either wells, the reservoir characterization is steered by various petrophysical parameters including calculation of volume of shale, porosity, permeability and hydrocarbon saturation. The thickness of the Lockhart Limestone is 50 m and 77 m in the Meyal-05P and Meyal-10P wells, respectively. In Meyal-05P and Meyal-10P wells, the average petrophysical parameters values and ranges are given as follows: volume of shale 48% and 20%; density porosity 1–5.6% and 1–31.7%; neutron porosity 1–23% and 1–42.9%; sonic porosity 1–29% and 1–39%; effective porosity < 1–> 5% and 1–21%; and hydrocarbon saturation 92.21–99.8% and 97–99.6%. The petrophysical parameters indicate that the Lockhart Limestone of Meyal-10P well is quantitatively better reservoir than that of the Meyal-05P. In Lockhart Limestone of either wells, the permeability is < 0.1 mD. The bulk volume water deciphered the presence of vuggy and intercrystalline porosity in the Lockhart Limestone. Similarly, the lithological interpretation using logs shows mainly limestone with minor shales. Different electrofacies are interpreted from the log trends of gamma ray log such as aggrading, prograding and retrograding depositional sequences deposited in tidal channel fill, shallow water, shore line and offshore buildup and regressive-to-transgressive shore face depositional setting.

Keywords Lockhart Limestone · Petrophysical logs · Meyal Oil Field · Reservoir properties · Transgressive–regressive sequences · Depositional environment

Introduction

Meyal Oil Field is positioned in District Attock in an active foreland fold and thrust belt in the Potwar sub-basin of the Upper Indus Basin (Fig. 1; Hasany and Saleem 2012). The Potwar sub-basin is an important hydrocarbon province of Pakistan and one of the mature areas explored for petroleum in the country (Kadri 1995). In 1915 at Khaur (District Attock), Punjab, commercial quantities of oil were discovered by the predecessor of Attock Oil Company (AOC) which founded the petroleum exploration history of the Potwar sub-basin (Kadri 1995). In 1968, Pakistan Oilfields Limited (POL) discovered the Meyal Oil Field. The Meyal Oil Field is one of the key oil producing fields in the Potwar sub-basin which includes 16 wells. It has produced over 36 MMB oil and 250 BCF gas from fractured Paleocene–Eocene shallow marine shelf carbonates of the Lockhart and Chorgali–Sakesar formations and Jurassic Datta sandstone (Hasany and Saleem 2012).

The Lockhart Limestone is well-exposed in Kohat-Potwar sub-basins, Salt Range, Trans-Indus ranges,

✉ Muhammad Awais
awais.geo@uoswabi.edu.pk

1 Department of Geology, University of Swabi, Anbar, Swabi, Khyber Pakhtunkhwa, Pakistan

2 Department of Geology, University of Malakand, Dir Lower, Khyber Pakhtunkhwa, Pakistan

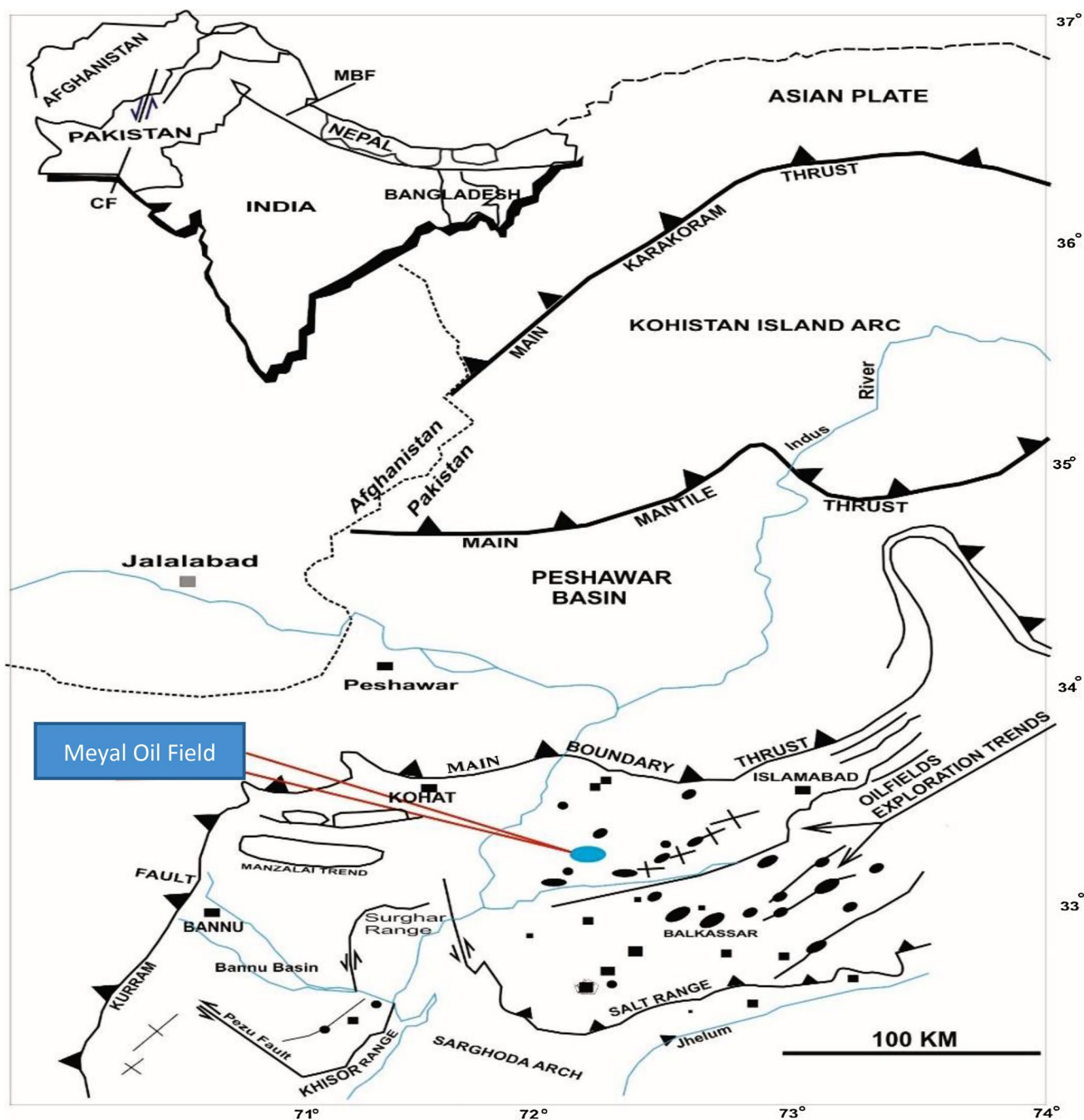3 Geological Survey of Pakistan, Quetta, Pakistan

Fig. 1 Regional map showing location and tectonic setting of the Meyal Oil Field (marked by blue ellipse). Modified after Kazmi and Rana (1982) and Hasany and Saleem (2012)

Kala-Chitta Range, Islamabad, and Hazara-Kashmir area(s) (Shah 2009). In the Kohat area, Lockhart Limestone consists of medium to thick bedded, massive, rubbly and brecciated limestone. In the Salt Range and Trans-Indus ranges, the Lockhart Limestone consists of medium bedded and nodular limestone with minor amounts of shale and marls. In the Hazara and Kala-Chitta areas, the Lockhart Limestone is comprised of dark-colored nodular and massive limestone and intercalations of shale and marl (Shah 2009; Awais et al. 2012 and 2013). The Lockhart Limestone has been studied extensively by earlier investigators (e.g., Afzal et al. 2005; Sameeni et al. 2009; Yaseen et al. 2011; Hanif et al. 2013; Sameeni et al. 2013; Ahmad et al. 2014; Malik and Ahmed 2014; Khan et al. 2016; Bilal and Khan 2017; Khattak et al. 2017) in the context of sedimentology, biostratigraphy

and sequence stratigraphy. Similarly, different researchers have investigated the diagenetic fabric of the Paleocene Lockhart Limestone exposed in the Kohat-Potwar sub-basins, Islamabad, Salt Range (central and western), Margalla Hill Range and Azad Kashmir (Ali et al. 2014; Khan et al. 2016; Bilal and Khan 2017; Khattak et al. 2017; Khan et al. 2018). However, no published work is available on reservoir characterization, sequence stratigraphy (T–R sequences) and depositional environment of the Lockhart Limestone penetrated in the Meyal-05P and Meyal-10P wells. According to Hasany and Saleem (2012), Lockhart Limestone consists of massive, argillaceous limestone in the Meyal Oil Field. The Lockhart Limestone is penetrated in few wells and is a heterogeneous quality reservoir thereby produced very limited hydrocarbons (Hasany and Saleem 2012). In the Hazara area, visually estimated 11% porosity is reported in the Lockhart Limestone (Nawaz et al. 2015). The Lockhart Limestone penetrated in the Chanda deep-01 well of the Kohat sub-basin has 9.5% porosity, 5.5% volume of shale and 70.6% hydrocarbon saturation and evinces good quality reservoir (Nawaz et al. 2015). According to Saddique et al. (2016), the Lockhart Limestone is dominated by limestone with 36 m thickness in Kahi-01 well, Kohat sub-basin, Pakistan. The limestone units are vacated by vuggy and crystalline porosities and are declared as a hydrocarbon bearing formation (Saddique et al. 2016). Ahsan and Shah (2017) have studied reservoir characteristics and depositional fabric of the Lockhart Limestone outcropped in the Hazara-Kashmir area(s). In the Hazara-Kashmir area(s), the porosity of the Lockhart Limestone ranges from 0.5% (tight) to 4% (Ahsan and Shah 2017). Ahsan and Shah (2017) reported nodular limestone and minor shales within the Lockhart Limestone of the Hazara-Kashmir area(s). The Lockhart Limestone is interpreted as carbonate ramp and represents retrogradational/ progradational (transgressive/highstand systems tract) stacking pattern (Ahmad et al. 2014; Ahsan and Shah 2017). Siyar et al. (2018) interpreted reservoir properties of the Paleocene Lockhart Limestone in Chanda-01 well, Kohat sub-basin, Pakistan. They have demarcated a reservoir zone within carbonates of the Lockhart Limestone having 4% volume of shale, 5% average porosity, 4% effective porosity and 85% hydrocarbon saturation.

It is obvious from the above discussion that no such work on the petrophysical properties in combination with sequence stratigraphy of the Paleocene Lockhart Limestone of Meyal Oil Field has been done before. The current research is an effort to investigate the reservoir suitability to establish the T–R (transgressive–regressive) sequences and to interpret the depositional setting of the Lockhart Limestone using the conventional petrophysical logs.

General geology

The Potwar sub-basin is situated in the lesser Himalayas of Pakistan, a zone of deformed meta-sedimentary and sedimentary rocks originally deposited on the northern Indian continental margin and in the Indo-Gangetic foreland basin (Fig. 1; Kazmi and Jan 1997). The northern and southern limits of the Potwar sub-basin are marked by Main Boundary Thrust (MBT) and Salt Range Thrust (SRT), whereas the eastern and western limits are marked by the left lateral Jhelum and the right lateral Kalabagh faults, together with Indus River, respectively (Fig. 1; Kazmi and Jan 1997). The Northern Potwar Deformed Zone (NPDZ) contains the Meyal Oil Field. Meyal Oil Field represents a structural trap and the main structure consists of east–west trending Meyal-Kharpa anticline (Fig. 2; Hasany and Saleem 2012). Meyal-Kharpa surface structure is an east–west trending narrow, steep, faulted anticline with two major thrusts cutting the structure longitudinally. At the Eocene level, the subsurface structure is defined as east–west trending pop-up, salt cored, doubly plunging, gentle dipping anticlinal fold bounded by thrust faults in the north and south (Fig. 2; Ghazi et al. 2014).

The geological formations in the selected wells (i.e., Meyal-05P and Meyal-10P) of the Meyal Oil Field vary in age from Triassic rocks to Pliocene Nagri Formation (Fig. 3). There are three unconformities, i.e., between Triassic Mianwali and Jurassic Datta Sandstone; between Datta Sandstone and Paleocene Hangu Formation; and between Eocene Kohat Formation and Miocene Murree Formation (Fig. 3). The Paleocene Makarwal group consists of Hangu, Lockhart and Patala formations. Among them, Lockhart Limestone is the target formation in the current research.

Materials and methods

The present study data set consists of conventional well logs (gamma ray, resistivity, caliper, density, neutron, sonic, spontaneous potential and Photoelectric Factor) of Meyal-05P (33°16′43″N; 72°08′01″E) and Meyal-10P (33°16′30″N; 72°10′54″E) wells (Figs. 1, 4). The petrophysical analyses were conducted manually using MS Excel with some usage of Geographix software. The gamma ray (GR) log is used to determine volume of shale, interpret lithology, to establish T–R sequences and depositional environments, in combination with the published literature. The lithology of the Lockhart Limestone is interpreted using GR, caliper, spontaneous potential (SP), neutron (NPHI), density (RHOB), sonic (DT) and PEF (Photoelectric Factor) logs.

The following formulae are used to calculate different petrophysical parameters, i.e., volume of shale, density porosity, sonic porosity and effective porosity, for the Lockhart Limestone (Rider 1996).
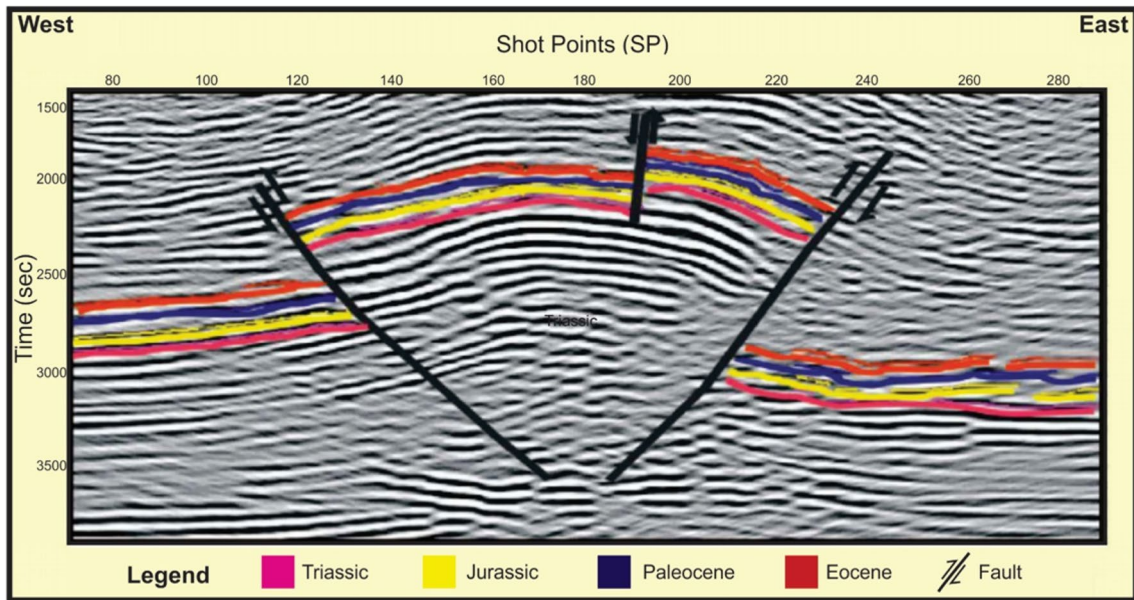
Fig. 2 Seismic section of line S97-MYL-06 showing pop-up structure in the Meyal Oil Field, Potwar Sub-basin, Pakistan (modified after Hasany and Saleem 2012; Ghazi et al. 2014)
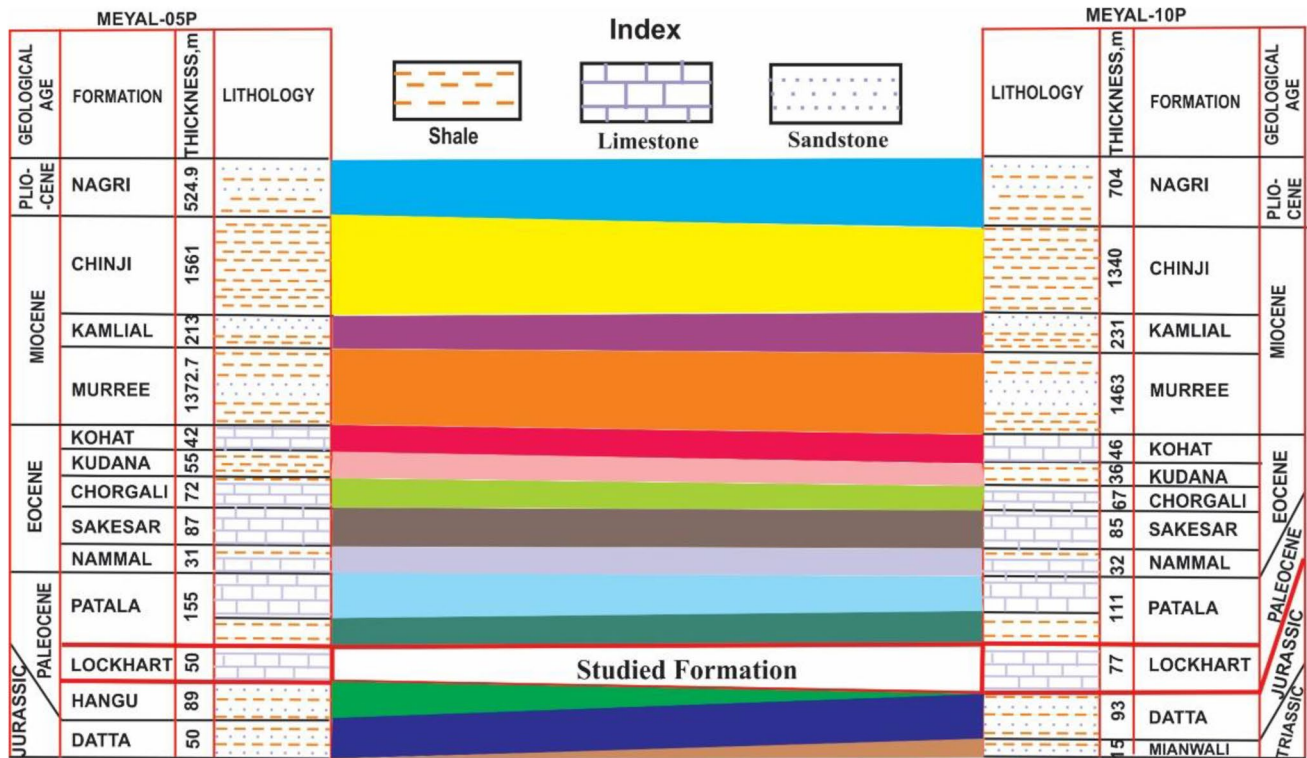

Fig. 3 Stratigraphic correlation chart of Meyal-05P and Meyal-10P wells, Meyal Oil Field
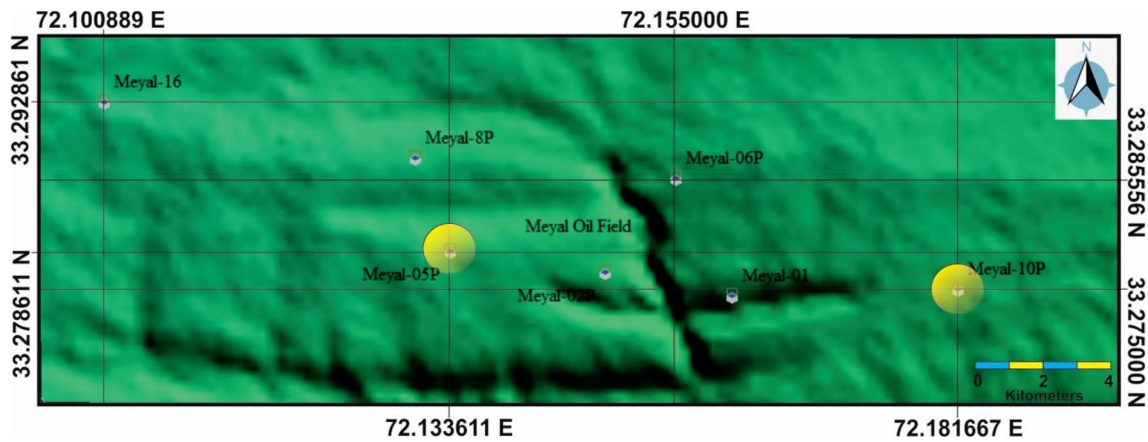
Fig. 4 Base map of wells generated on digital elevation model (DEM) data of the Meyal Oil Field. The studied wells are encircled in yellow color

Volume of shale (%) $= V_{sh} = \dfrac{GR(log) - GR(min)}{GR(max) - GR(min)}$ (1)

Density porosity $= \Phi D = \dfrac{\rho_{ma} - \rho_b}{\rho_{ma} - \rho_f}$ (2)

Sonic porosity $= \Phi_s = \dfrac{\left(\Delta t \, log - \Delta t_{ma}\right)}{\left(\Delta t_f - \Delta t_{ma}\right)}$ (3)

Effective porosity $= \Phi_{eff} = \Phi_{Total} \times \left(1 - C \times V_{sh}\right)$ (4)

Timur permeability equation is used to find out the permeability, given in Eq. (5).

Permeability $K = (93 * \varnothing a^{2.2} / S_w)^2$ (5)

where GRlog stands for GR log reading; GRmax and GRmin represent maximum GR log and minimum GR log in API; ρ_b, ρ_{ma} and ρ_f are density reading from log, matrix density and fluid density in gm/cc; Δtlog and Δt_{ma} are interval transit time from log and interval transit time of matrix, respectively, and Δt_f denotes interval transit time of fluids in μs/ft; Φ_{Total} is total porosity, Φ_{eff} is effective porosity and C is constant in the equation of effective porosity; and $\varnothing a$ is average porosity, and 'S_w' is water saturation.

Calculation of hydrocarbon saturation

In order to calculate the water saturation (S_w), first we have to know about resistivity of water (R_w), and then using Archie equation, the water saturation (S_w) can be calculated (Rider 1996).

$S_w = \left[\left(\dfrac{a}{\Phi^m}\right)\left(\dfrac{R_w}{R_t}\right)\right]^{1/n}$ (6)

where S_w = water saturation; R_w = water resistivity; Φ = porosity; m = cementation factor; a = tortuosity factor; R_t = log response (LLD)

R_w can be computed by the following method involving calculation of temperature (T) of the formation (Fm).

Average temperature of Formation
$=$ Surface Temperature $+$ Bottom Temperature/2 (7)

where Temperature at the top of Formation = Formation Top × Temperature Gradient + Surface Temperature, Temperature at the Bottom of Formation = Formation Bottom × Temperature Gradient + Surface Temperature.

Temperature gradient is calculated from Eq. (8).

Temperature Gradient $=$ Maximum BHT
$-$ Surface Temperature/Total Depth (TD) (8)

In the present study, the calculated values of different temperatures and formation top and bottom for Lockhart Limestone of Meyal-05P includes Bottom Hole Temperature (BHT) = 56.11 °C; Surface temperature = 25 °C; Formation top = 4107.2, and Formation bottom = 4157.8 m. Hence, the calculated temperature gradient is 0.0130 °C. Also temperature at the top and bottom of the formation is 130.3936 °C and 131.0514 °C, respectively. Putting the value of temperature gradient in Eq. (8), the formation temperature (T_f) is calculated to be 55 °C. The Schlumberger (2009) chart is used to calculate the values of Rmf (0.27 Ω m), Rmfeq (0.23 Ω m) and R_w (0.21 Ω m) (Fig. 5). Similar method is also followed for Meyal-10P.

Hydrocarbon saturation has been calculated using the following equation (Rider 1996);

$S_{hc} = 1 - S_w$ (9)

where S_{hc} is hydrocarbon saturation and S_w is water saturation.
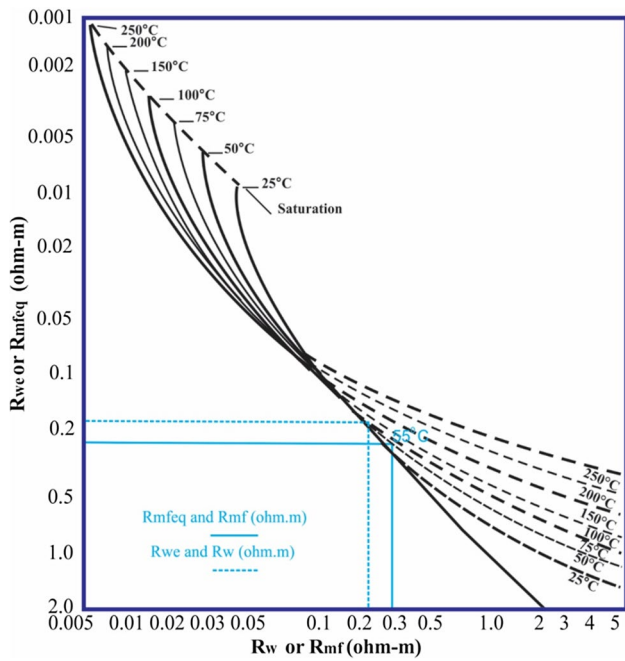
Fig. 5 Schlumberger chart showing Rmf, Rmfeq and Rwe and R_w values at formation temperature for Lockhart Limestone of Meyal-05P (modified after Schlumberger 2009)

Table 1 Carbonates porosity types $V_b \cdot w$ values (Fertl and Vercellino 1978)

Carbonates porosity types	$V_b \cdot w$ values
Vuggy	0.005–0.015
Vuggy and intercrystalline (intergranular)	0.015–0.025
Intercrystalline (intergranular)	0.025–0.04
Chalky	0.05

Bulk volume of water ($V_b \cdot w$) is the proportion of the total rock volume occupied by water (Rider 1996). In carbonates, $V_b \cdot w$ values helps in the interpretation of different types of pores present in the rock (Table 1; Fertl and Vercellino 1978). In the present study, the porosity types in Lockhart Limestone are interpreted based on $V_b \cdot w$. $V_b \cdot w$ can be calculated from well logs using the following equation (Rider 1996):

$$V_b \cdot w = \phi_{eff} \times S_w \qquad (10)$$

Results and discussion

The Lockhart Limestone penetrated in Meyal-05P and Meyal-10P wells is investigated in the context of well logs-based reservoir evaluation, establishment of T–R (transgressive–regressive) sequences and interpretation of depositional environments. The thickness of the formation is 50 meters (m) and 77 m in the Meyal-05P and Meyal-10P wells, respectively (Figs. 3, 6). It implies that the thickness of the carbonates is increasing toward the eastern side of the study area (Figs. 3, 6).
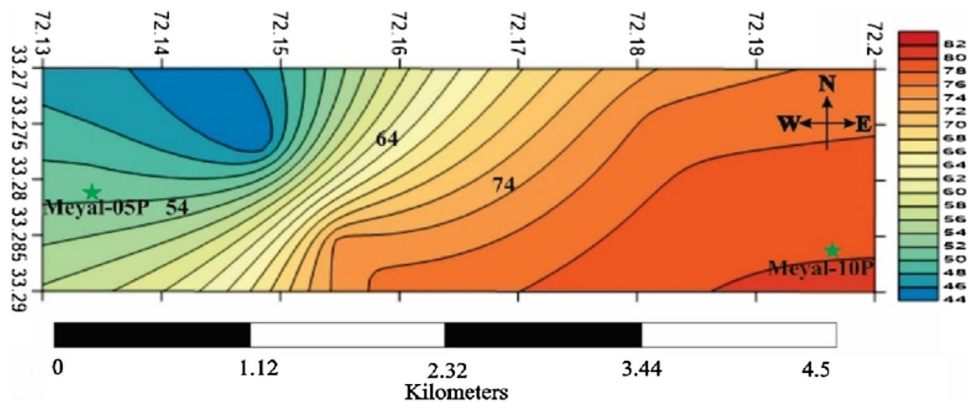
Petrophysical analysis of the Lockhart Limestone of Meyal-05P well

In the Meyal-05P, the Lockhart Limestone starts at depth of 4107.2 m and ends at 4157.8 m. Different petrophysical logs have been run through this interval, and the following formation evaluation parameters are measured from these logs (Fig. 7).

Volume of shale (V_{sh})

The average volume of shale in the Lockhart Limestone of Meyal-05P is 48 percent (%). Following Ghorab et al. (2008), the Lockhart Limestone is divided into three zones based on the volume of shale, i.e., shale zone containing > 35% shale (eight intervals); shaly zone containing 10–35% shale (seven intervals), and clean zone containing < 10% shale (one interval) (Fig. 8).

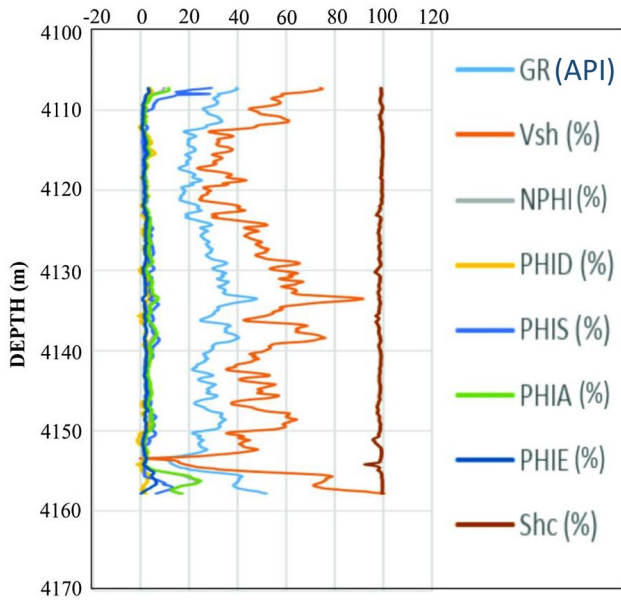**Fig. 6** Isopach map of the Lockhart Limestone showing its thicknesses in Meyal-05P and Meyal-10P wells

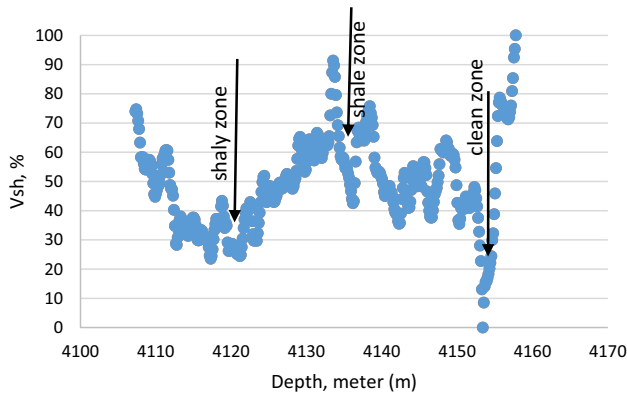**Fig. 7** Petrophysical logs of the Lockhart Limestone of Meyal-05P well

Fig. 8 Shale, shaly and clean zones within the Lockhart Limestone of Meyal-05P, Meyal Oil Field

Fig. 9 Effective porosity of the Lockhart Limestone of Meyal-05P, Meyal Oil Field
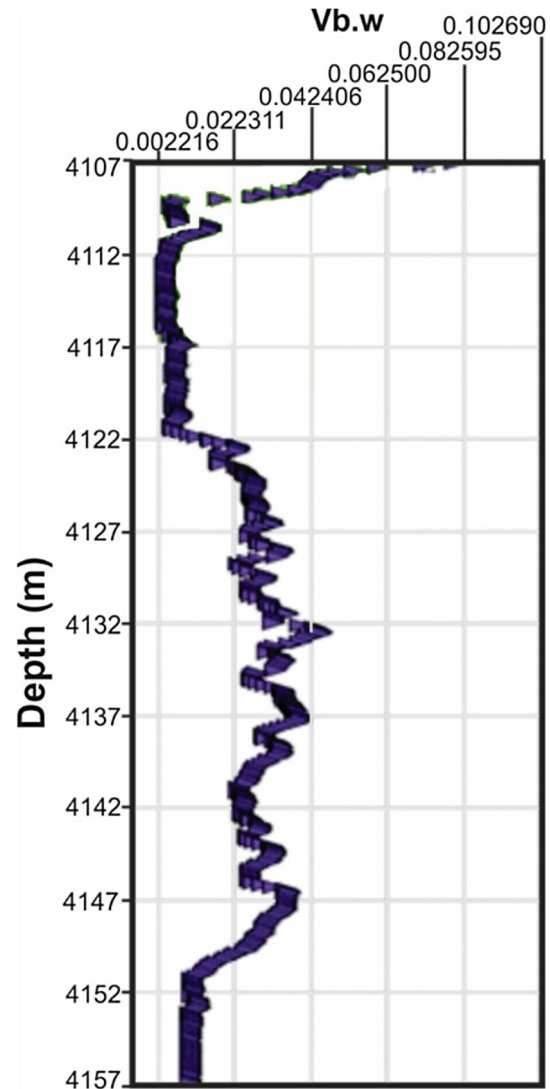
Fig. 10 Cross-plot showing the bulk volume of water (Vb.w) with respect to depth

Porosity

Porosity is calculated from different logs such as density, neutron and sonic logs. The density porosity ranges from 1 to 5.6% (Fig. 7). The neutron porosity ranges from 1 to 23% (Fig. 7). The sonic porosity varies from 1 to 29% (Fig. 7). The term "effective porosity" or "connected" pore space is commonly used to denote porosity that is mostly available for fluid flow. However, at certain scale all pore spaces are connected (Lucia 2007). In the Lockhart Limestone of Meyal-05P, the effective porosity is in the range of < 1–> 5% (Fig. 9).

In Meyal-05, major portion of $V_b \cdot w$ lies in the range of 0.025–0.04 (54%) reflecting the presence of intercrystalline

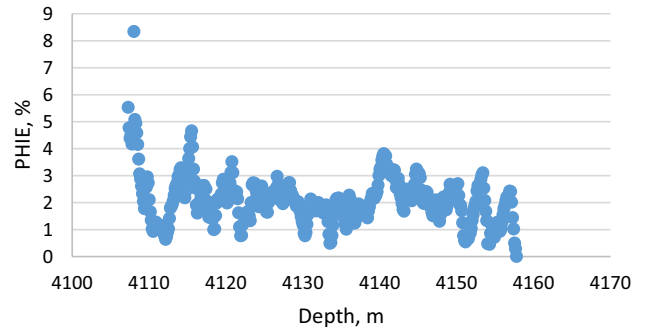porosity in the Lockhart Limestone (Fig. 10). Similarly, Vb.w also ranges from 0.005 to 0.015 (31%) and 0.015–0.025 (13.5%) evidencing the presence of vuggy, and vuggy-intercrystalline porosity (Fig. 10).

Hydrocarbon saturation

The interval of the Lockhart Limestone that is drilled in the Meyal-05P well contains a desirable amount of hydrocarbons. The value for hydrocarbon saturation lies in the range of 92.21–99.8% (Fig. 7).

Petrophysical analysis of the Lockhart Limestone of Meyal-10P well

In the Meyal-10P, the Lockhart Limestone starts at depth of 4118.5 and ends at 4195.3 m. The fundamental logs have been run in this interval and the following petrophysical parameters have been calculated from these logs (Fig. 11). Details of these petrophysical parameters are given below.

Volume of shale

In the Meyal-10P well, the average volume of shale in the Lockhart Limestone is 20%. Following Ghorab et al. (2008), the Lockhart Limestone is divided into three zones based on the volume of shale, i.e., shale zone containing > 35% shale (06 intervals with thicknesses ranging from 01 to 03 m); shaly zone containing 10–35% shale (19 intervals with thicknesses varying from 1 to 22 m) and clean zone containing

< 10% shale (13 intervals with thicknesses ranging from 1 to 4 m) (Fig. 12).

Porosity

The density porosity ranges from 1 to 31.7% (Fig. 11). The neutron porosity ranges from 1 to 42.9% (Fig. 11). The sonic porosity varies from 1 to 39% (Fig. 11). Likewise, the effective porosity is in the range of 1–21% (Figs. 11, 13).

In Meyal-10P, most of the values for the $V_b·w$ lie in the range of 0.015 and 0.025 (26.70%) which show the presence of vuggy and intercrystalline porosity. Also many values fall in the range of 0.025 and 0.04 (25.10%) which is an indication of intercrystalline porosity. Few values are ranging between 0.005 and 0.015 (5.50%) reflecting the vuggy porosity.

Hydrocarbon saturation

This interval of Lockhart Limestone contains a desirable amount of hydrocarbons, i.e., 97–99.6% (Fig. 11).
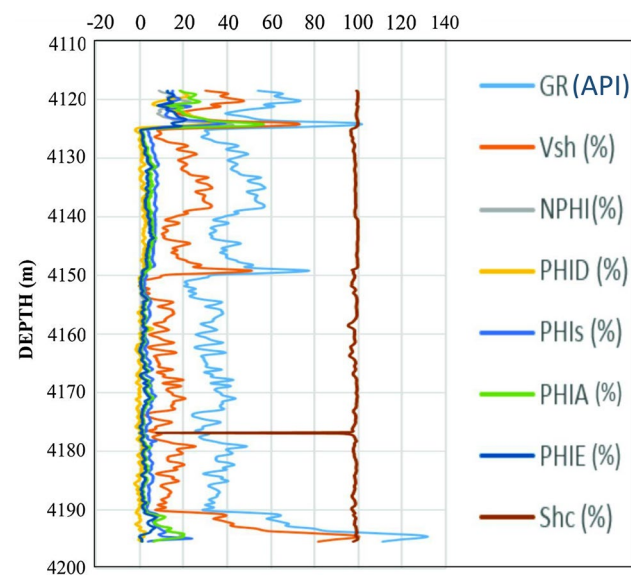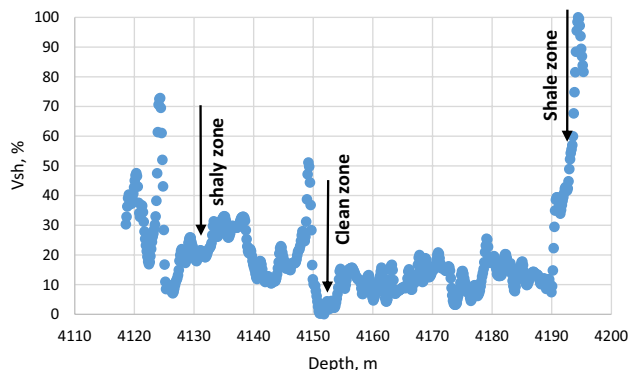
Fig. 12 Shale, shaly and clean zones within the Lockhart Limestone of Meyal-10P, Meyal Oil Field

Fig. 13 Effective porosity versus depth of the Lockhart Limestone of Meyal-10P, Meyal Oil Field

Fig. 11 Petrophysical logs of the Lockhart Limestone of Meyal-10P well, Meyal Oil Field

Table 2 Qualitative assessment of porosity for a reservoir (Rider 1996)

Qualitative assessment of porosity	
Average porosity (%)	Qualitative description
0–5	Negligible
5–10	Poor
10–20	Good
20–30	Very good
>30	Excellent

Permeability (K)

The permeability is calculated from the Timur Permeability equation which is less than 0.1 mD (millidarcy) for the Lockhart Limestone of both Meyal-05P and Meyal-10P wells.

Based on the quantitative parameters, Lockhart Limestone of Meyal-10P is a good reservoir as compared to that of Meyal-05P. In Meyal-05P and Meyal-10P wells, the average volume of shale is 48% and 20%; the range of density porosity is 1–5.6% and 1–31.7%; range of neutron porosity is 1–23% and 1–42.9%; the range of sonic porosity is 1–29% and 1–39%; the range of effective porosity is <1–>5% and 1–21%; and the range of hydrocarbon saturation is 92.21–99.8% and 97–99.6%. Following Rider (1996) reservoir quality based on porosity values, the Lockhart Limestone of Meyal-05P well is a poor reservoir; however, the Lockhart Limestone of Meyal-10P well is a very good reservoir (Table 2; Figs. 7, 9, 11, 13). In Lockhart Limestone of either wells, the permeability is <0.1 mD. Hence, based on the very low permeability (<0.1 mD) and very high hydrocarbon saturation, the Lockhart Limestone is interpreted to be a tight reservoir. In order to get precise results, log-to-core calibration is an important step; however, cores were not available for the present study.

Diagenetic fabric and reservoir quality of the Lockhart Limestone: Petrographic approach

The changes in petrophysical parameters with the changes in porosity are concerned with the diagenetic processes in carbonates (Fig. 14; Anselmetti and Eberli 1997). Porosity is controlled by diagenetic features like cementation, neomorphism, micritization, compaction, dissolution, dolomitization and fracturing (Flügel 2010; Fig. 15). In the Margalla Hill Range, the Lockhart Limestone is diagenetically altered into stylobreccia, stylolaminated, stylonodular, stylolite and fractured fabric (Khan et al. 2018). According to Bilal and Khan (2017), the Lockhart Limestone, outcropped in Azad Kashmir, has experienced micritization, dolomitization,
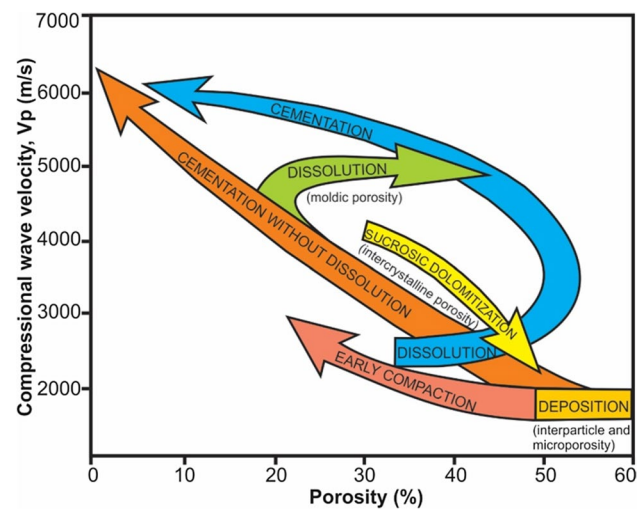

Fig. 14 Velocity-porosity paths of various diagenetic processes in carbonate sediments. Any given process may have a different position on the diagram depending on the timing of the diagenetic events, but the trend (direction of arrow) should be the same (after Anselmetti and Eberli 1997)

neomorphism, cementation, compaction and fracturing. In Islamabad, Khattak et al. (2017) reported different diagenetic features in the Lockhart Limestone such as mechanical and chemical compaction, deep burial water pressure, pressure solution and tectonics-related fracturing. In the Kohat area, the diagenetic alterations of the Lockhart Limestone include tight packing, stylolitization, dolomitization, neomorphism (aragonite to calcite transformation) and spar-filled fractures (Fig. 15a, b, d, f; Ali et al. 2014; Khan et al. 2016). Along Nathiagali-Murree Road (District Abbottabad) outcrop section, the Lockhart Limestone diagenetic fabric is characterized by micritization, neomorphism (aragonite to calcite alteration), compaction, stylolitization, calcite-filled microfractures, development of microspar and nodularity (Fig. 15a; Ali et al. 2014).

Different porosity types are reported based on the $V_b \cdot w$ values for carbonates of the Lockhart Limestone. In this connection, it is also worth mentioning that intergranular, vuggy, moldic and fracture type of porosities are reported through petrographic studies by Ahmad et al. (2014) in the Lockhart Limestone of the Nammal Gorge, Western Salt Range, Pakistan (Fig. 15c, e). There are variations in the values of density, neutron and sonic log porosities. All the porosity logs, i.e., density, neutron and sonic logs estimate both primary and secondary porosities. In fact, the porosity is not directly measured by these logs but they consider the physical parameters of the formation and link them to porosity estimation using mathematical calculations (Rider 1996). The density and neutron logs consider pore spaces of all sizes. Sonic log measures the interparticle/intergranular/intercrystalline primary porosity and is less sensitive
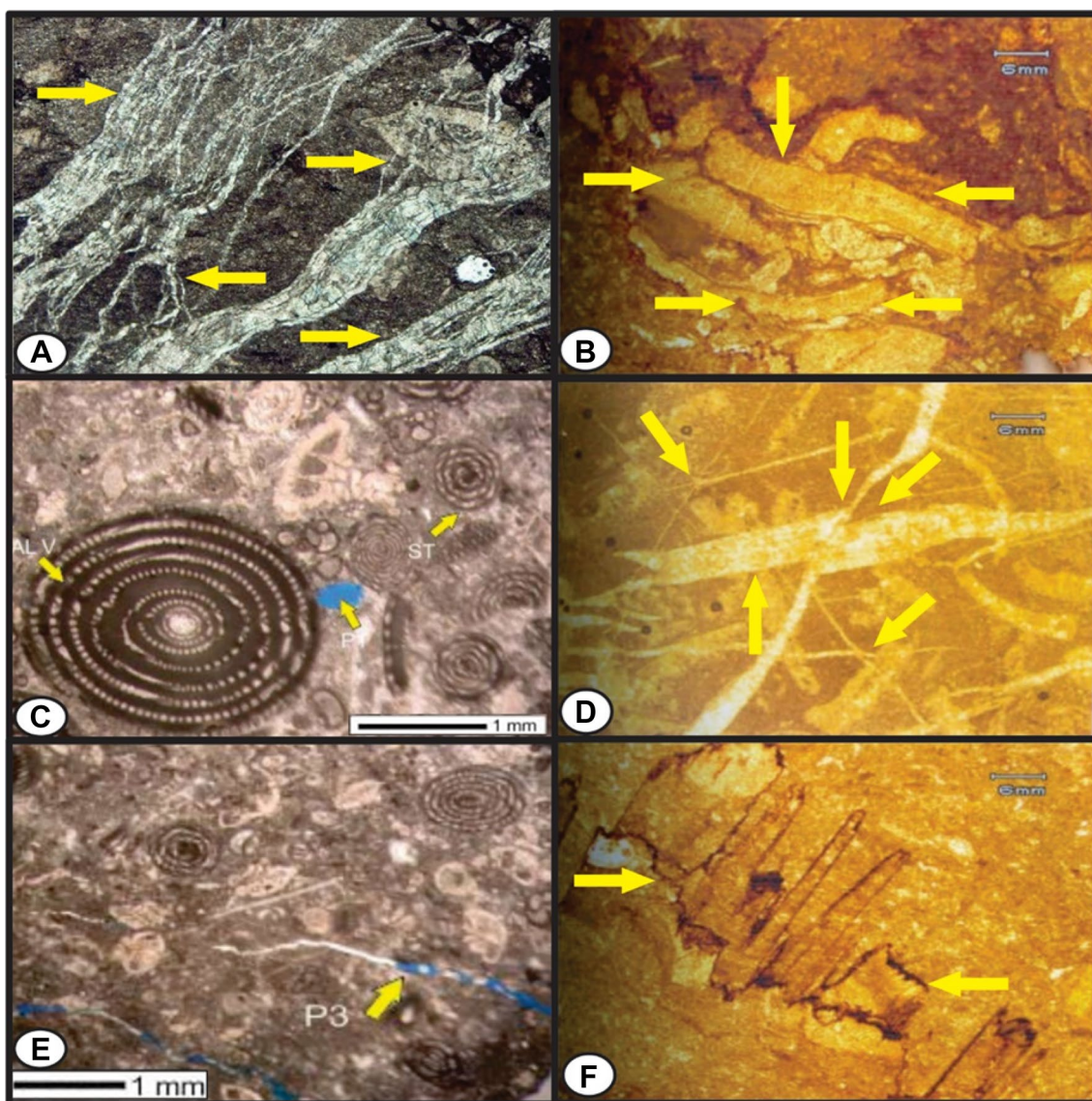
Fig. 15 Photomicrographs of diagenetic features within the carbonates of the Lockhart Limestone **a** Parallel sets of calcite-filled microfracture (arrowhead) swarms intersecting Lockhartia sp. (top right). These calcite-filled microfracture swarms seem to be the result of hydraulic fracturing of Lockhart Limestone (Plane polarized light, Mag. ×4) (Ali et al. 2014); **b** Tight fabric of allochemical constituents, attributed to phenomena of post depositional pressure dissolution; Cross polarized light (XPL); **c** Lockhart Limestone having vuggy porosity (P1). ALV for Alveolina globula and ST for stylolite; **d** Lockhart Limestone characterized by multiple set of calcite filled fractures (XPL); **e** Lockhart Limestone having fracture porosity (P3); **f** Microstylolites with high amplitude sutured fabric. Note truncation of depositional fabric along pressure-dissolution surface (XPL). **b**, **d** and **f** from Khan et al. 2016; **c** and **e** from Ahmad et al. 2014

for demarcating fractures and vugs, i.e., secondary porosity (Rider 1996). Furthermore, sonic log in combination with total porosity logs, i.e., density or neutron-density combo can be used to determine secondary porosity (Rider 1996).

Lithology interpretation of the Lockhart Limestone using petrophysical logs

The GR log of the studied wells is used to demarcate the shale and carbonates (reservoir) intervals within the Lockhart Limestone. A vital gizmo of lithology interpretation is density log when utilized in mishmash with neutron log. The combo of density and neutron logs is commonly used to divide limestone and dolostone in a carbonate succession. For limestone, the density and neutron logs will overlay and will be apart for dolostone, provided the correct log scale (Lucia 2007).

Within the Lockhart Limestone of the selected wells, the shale intervals are defined above 75 API, while the reservoir units are defined below 75 API (Fig. 16). The reservoir units

are also divided using the neutron-density combo. For shale interpretation using the neutron-density combo, the neutron value is high to the left compared to the density making a gap provided the GR curve is above 75 API. For demarcating the reservoir zones, the neutron-density logs for limestone overlays, while for dolostones, the neutron-density shows some gap having high neutron value to the left compared to the density value provided the GR curve is below 75 API (Rider 1996).

In Meyal-05P, the lithology is interpreted to be dominantly limestone because the GR log is below the shale baseline throughout the interval (Fig. 16). The caliper log response is also very uniform, i.e., approximately lying at 7 inches throughout the interval. The SP log curve is almost straight without any prominent deflection reflecting the presence of clean limestone. The resistivity logs (SN, LLS and LLD) show higher values and away from each other. According to Rider (1996), the density log value for limestone is 2.71 g/cc, and likewise throughout the interval, the density log values are uniform, i.e., approximately at 2.71 g/cc. The sonic log values are also close to the matrix transit time for limestone (Fig. 16).

In Meyal-10P, the lithology is interpreted to be dominantly limestone but together with some minor shale because the GR log is below the shale baseline throughout the interval; however, at the shale interval, the GR log response is above the shale baseline (Fig. 17). The GR log response has fluctuations but it is below the shale baseline. The caliper log response varies from 6 to 7.5 in. with some local fluctuations might be due to argillaceous content in the limestone. The SP log curve is almost straight in the top and bottom of the interval demonstrating the availability of limestone (low qualitative permeability or impermeable) and very minor shale. However, it is deflected towards the negative SP values in the middle of the interval and therefore demarcates the presence of somewhat permeable limestone. The resistivity log (LLS) show higher values. Throughout the Lockhart Limestone, the neutron-density logs overlap each other, except at the shale intervals, thereby showing the presence of limestone. The sonic log values are also close to the matrix transit time for limestone (Fig. 17). The PEF log curve almost fall in the range of limestone value (i.e. ~ 5 barns/electron) throughout the formation having minor fluctuations might be due to variations in limestone composition and the presence of minor shale intervals in the upper and lowermost part of the formation (Fig. 17).

Transgressive–regressive (T–R) sequences for the Lockhart Limestone of Meyal-05P and Meyal-10P

Sequence stratigraphic analysis using petrophysical logs is an important component of analyzing a subsurface data set. Log data allow lithology and depositional environment to be integrated with the seismic section, thus linking seismic facies, rock properties and sedimentological facies. A number of studies have been made on sequence stratigraphy interpretation using petrophysical logs but the early one is that of Wagoner et al. (1990). Later on, other publications have also been presented by different authors (Vail and Wornardt 1990; Armentrout et al. 1993; Bowen et al. 1993).

Trends in log response (at any scale) therefore may equate with trends in depositional energy, and thus with patterns of sedimentary infill. The studies of Vail and Wornardt (1990) and Armentrout et al. (1993) showed that the key sequence stratigraphic surfaces (sequence boundary, maximum flooding surface and transgressive surface) could be located by interpreting the trends of the petrophysical logs. These trends indicate the relative sea-level position on the basis of which sedimentary fill can be divided into cycles (Fig. 18; Kendall 2003).

In Meyal-05P, the Lockhart Limestone is composed of five intervals as described from well log trends (Fig. 19). Starting from the top of the formation, a 4-m-thick interval-1 (bell shape) is present which shows the small variation from the fine toward the coarse, i.e., shale to non-shale/reservoir rock unit (Fig. 19). Below this interval, a 21-m-thick interval-2 of cylindrical shape is present underlain by a 5-m-thick rough bell shape interval-3 which shows fining upward sequence (Fig. 19). Interval-4 shows cylindrical trend indicating aggrading depositional sequence. At the bottom of the formation, a 5-m-thick interval-5 (funnel shape), coarsening upward sequence, is present (Fig. 19).

On the basis of different log trends of GR log, the Lockhart Limestone penetrated in the Meyal-10P is divided into five intervals (Fig. 20). Starting from the top of the Lockhart Limestone in the Meyal-10P well, a 5-m-thick interval-1 is demarcated showing coarsening upward funnel shape sequence and then fining upward sequence underlain by 2-m symmetrical interval. It is underlain by 14-m-thick funnel shape interval-2 showing coarsening upward sequence (Fig. 20). Then, a 10-m-thick symmetrical interval-3 is present which is underlain by 40-m-thick cylindrical interval-4. At the bottom of the formation, 5-m-thick funnel shape coarsening upward sequence (i.e., interval-5) is demarcated (Fig. 20; Kendall 2003).

Petrophysical log-based depositional facies (electrofacies) of Lockhart Limestone of Meyal-05P and Meyal-10P

The sequence stratigraphy is well-developed from electrofacies which are characterized by distinctive properties differ from the adjacent facies (Serra 1985). Such type of facies for
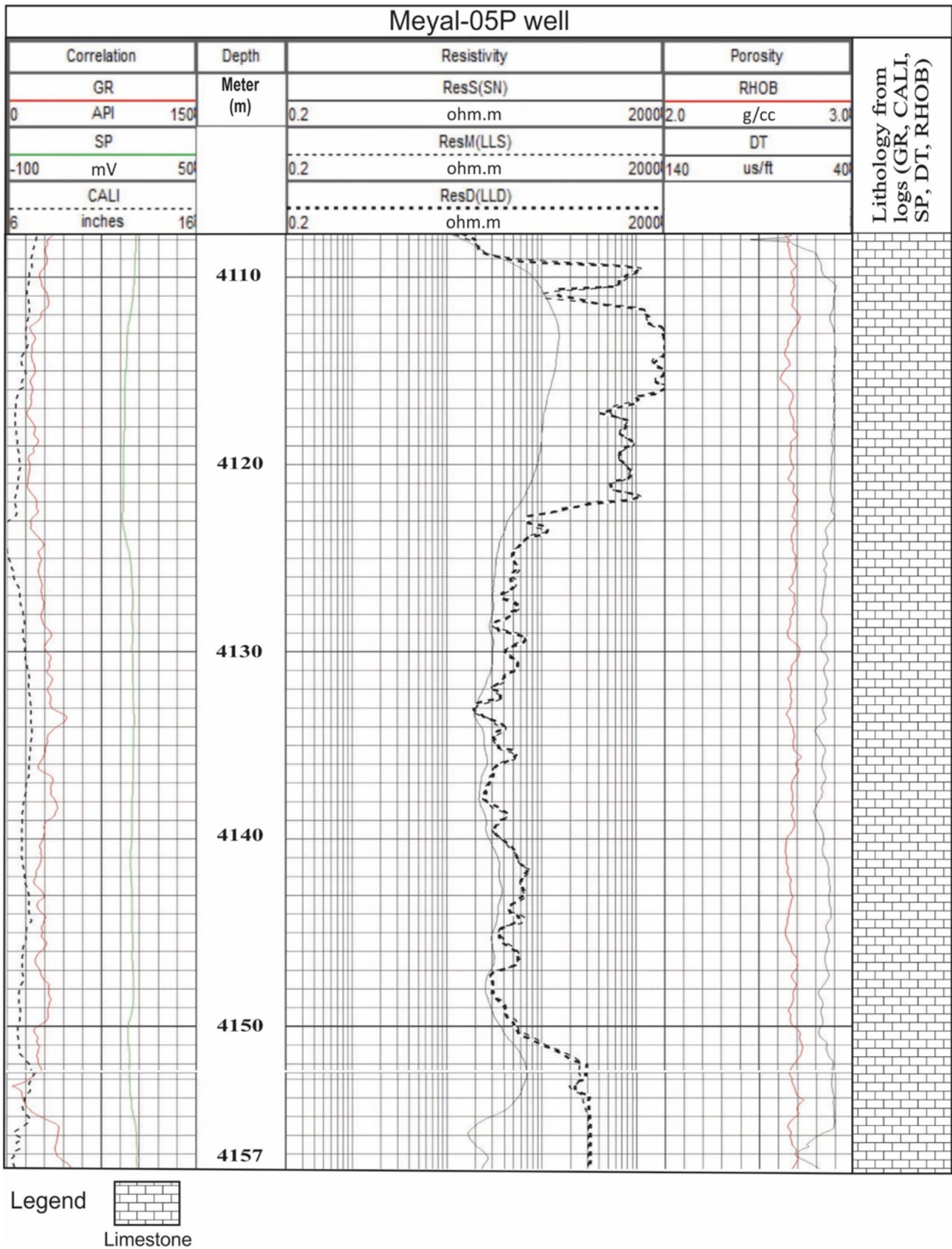
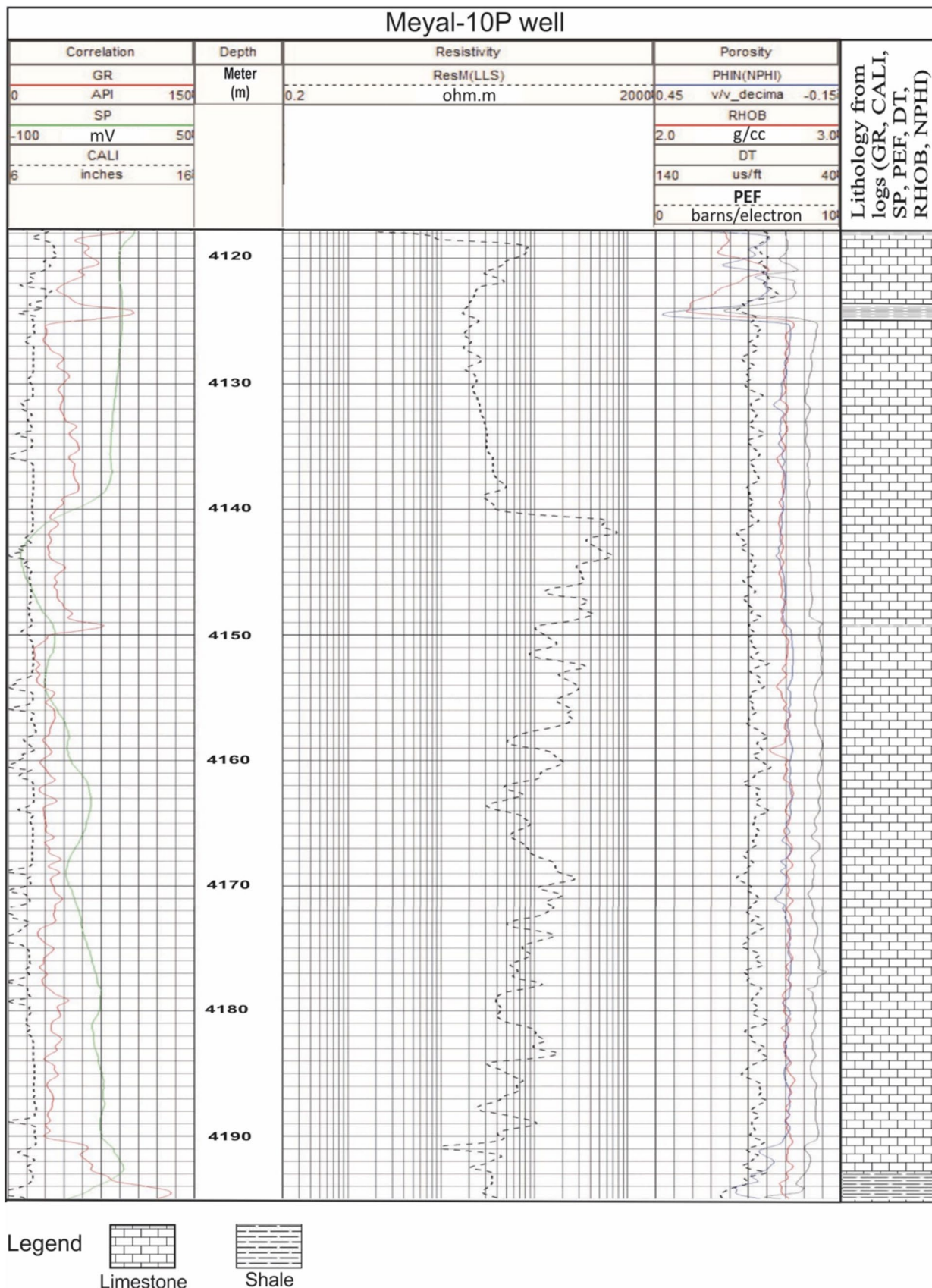**Fig. 16** Lithology interpretation of the Lockhart Limestone of Meyal-05P from petrophysical logs

Fig. 17 Lithology interpretation of the Lockhart Limestone of Meyal-10P from petrophysical logs
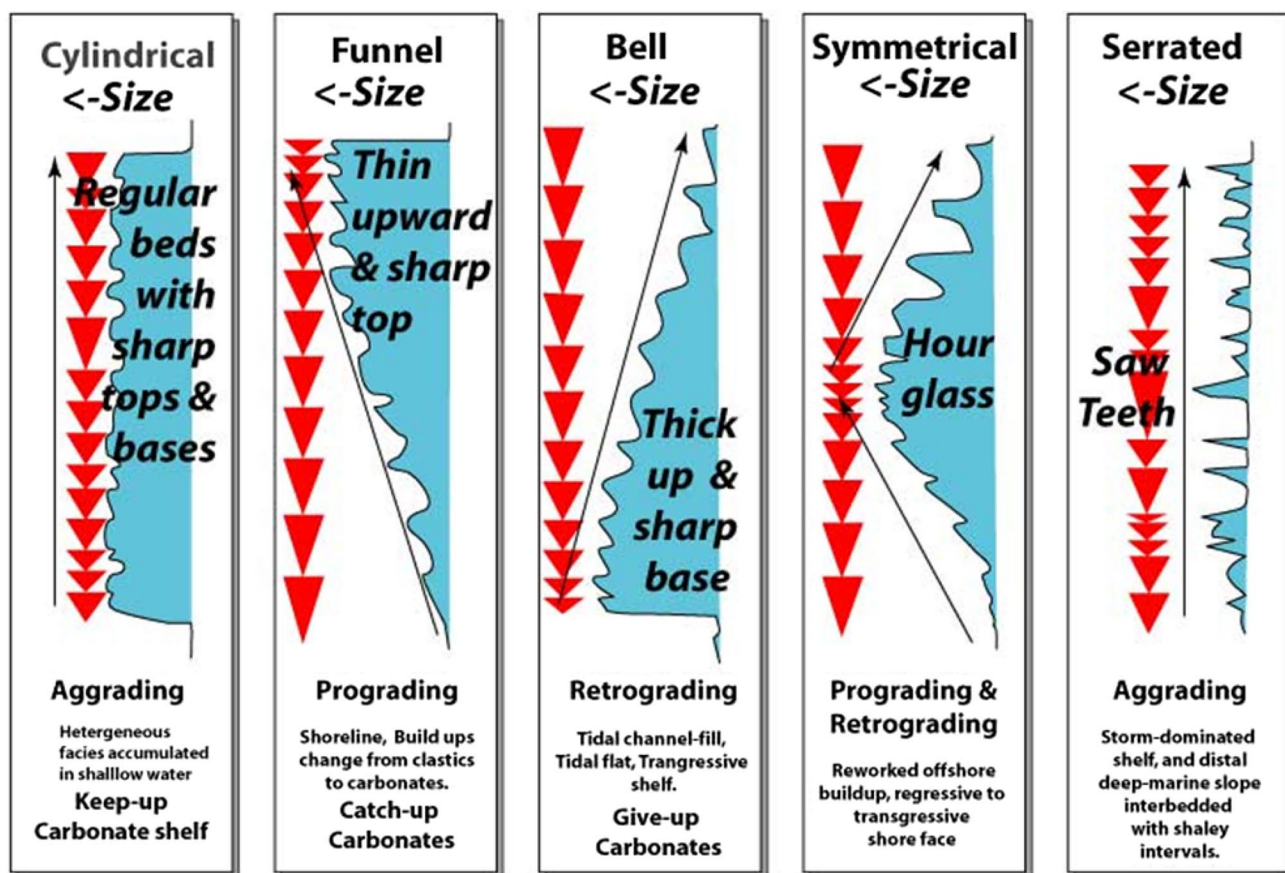
Fig. 18 Carbonates stacking patterns based on GR log trends (Kendall 2003)

the Lockhart Limestone in the Meyal-05P and Meyal-10P wells have been discussed in the below section.

Different electrofacies within the Lockhart Limestone of Meyal-05P interpreted from different log trends (GR, SP, LLD and RHOB) are discussed below.

Electrofacies 1 This is 4-m-thick (4107–4112 m) fining upward sequence indicating the retrogradational sequence (Figs. 19, 21). The GR log values undergo a small variation from the high value to the low values, while the resistivity log values increased from low to the high value. SP and density log values remain same. This trend indicates the depositional setting for the catch-up carbonates at the tidal channel fill, tidal flat (Figs. 19, 21; Kendall 2003).

According to the investigation of Malik and Ahmed (2014) on the Lockhart Limestone of Samana Range and Daud Khel sections, the facies assemblages correspond to inner platform/lagoon, platform margin and slope settings which show deposition in the inner, middle and outer parts of platform in supratidal, intertidal and subtidal environments. Hanif et al. (2013) interpreted inner ramp lagoon, shoal and fore-shoal open marine facies associations represented by wackestone and packstone foraminiferal–algal deposits within the Lockhart Limestone. These facies are

present in a cyclic order and displayed a retrograding carbonate ramp indicating the Thanetian transgressive deposits associated with eustatic sea-level rise (Hanif et al. 2013).

Electrofacies 2 This is 21-m-thick (4112–4133 m) unit having cylindrical shape indicating the aggradational sequence (Figs. 19, 21). The GR log values almost remain the same, while the resistivity log values first increased and then decreased. SP and density logs values remain same. This trend indicates the depositional setting for the keep-up carbonate at the shallow water (Figs. 19, 21; Kendall 2003).

According to Ahmad et al. (2014), three facies associations are recognized in downslope, along a distally steepened carbonate ramp platform. These facies associations correspond to inner ramp, middle ramp and ramp slope settings. The biostratigraphy implies that ramp carbonates were deposited in a single third-order depositional cycles in a highstand systems tract (Ahmad et al. 2014).

Electrofacies 3 This is 5-m-thick (4133–4137 m) rough bell shape fining upward sequence (Figs. 19, 21). The GR values for this interval go through a small variation from high value toward the lower value. While the values of density, resistivity and SP logs almost remain the same. This
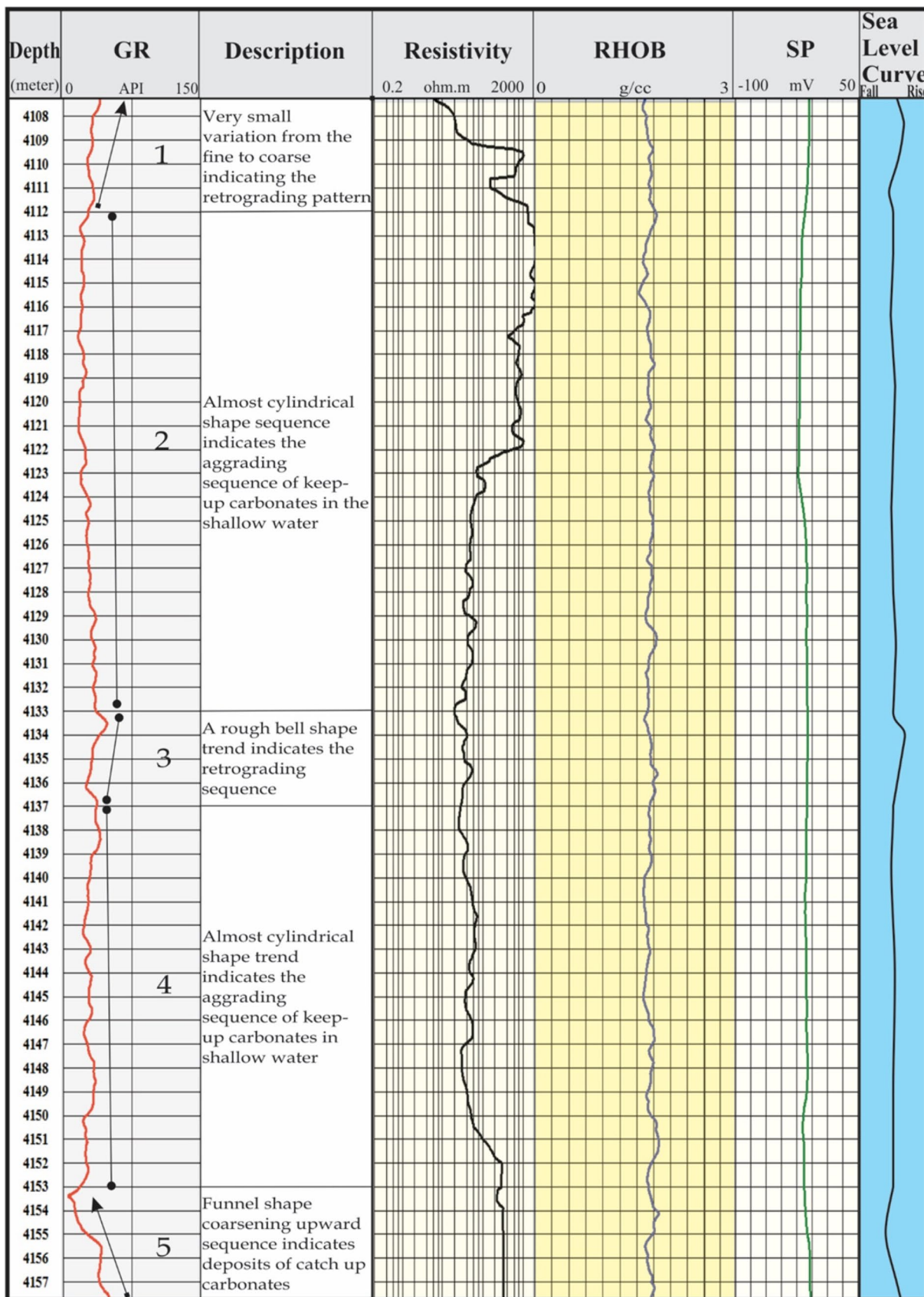
Fig. 19 Log response, depositional facies (electrofacies) and transgressive–regressive (T–R) sequences of the Lockhart Limestone in Meyal-05P
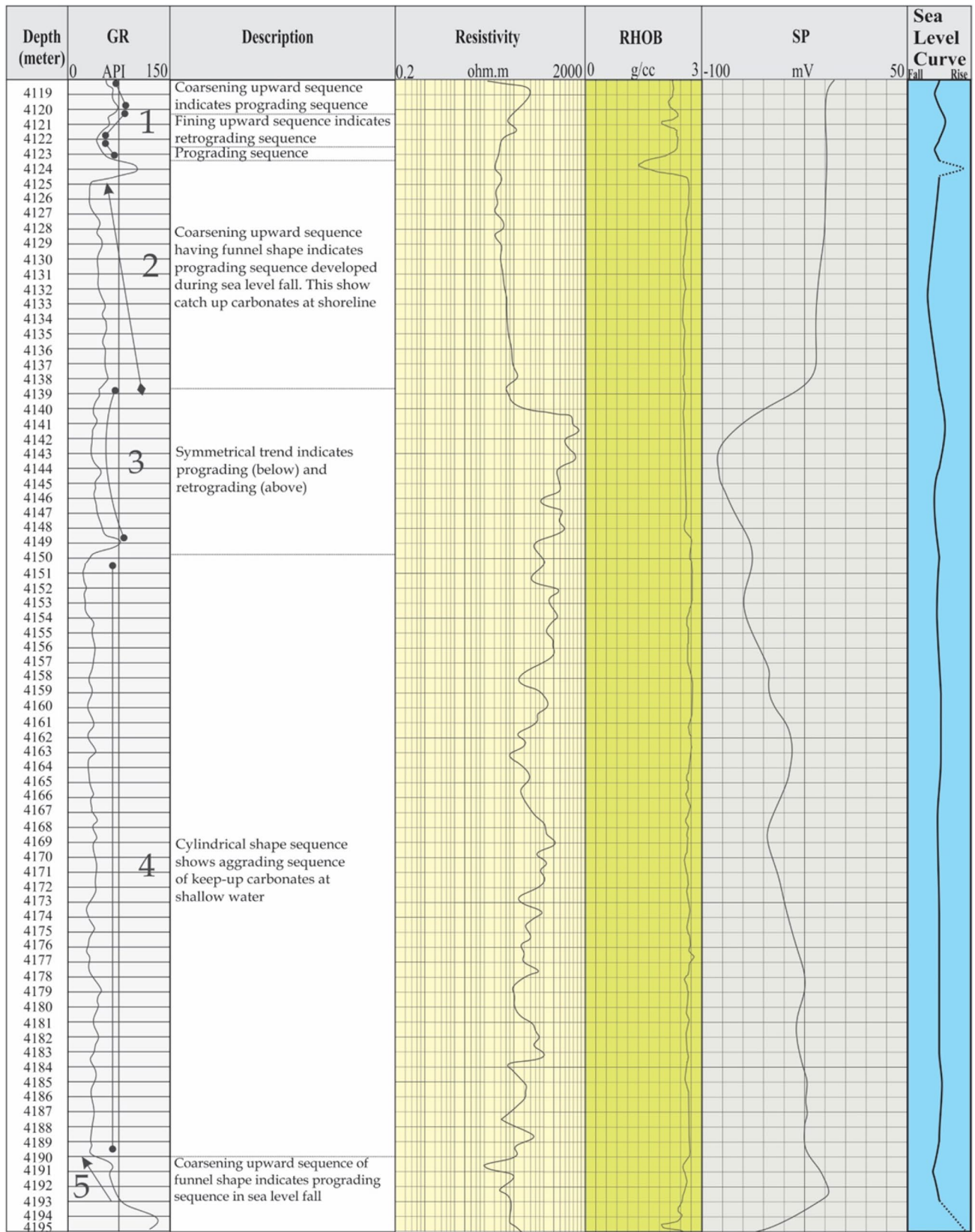
Depth (meter)	GR	Description	Resistivity	RHOB	SP	Sea Level Curve
	0 API 150		0.2 ohm.m 2000	0 g/cc 3	-100 mV 50	Fall Rise

Description column (top to bottom):

1 — Coarsening upward sequence indicates prograding sequence
Fining upward sequence indicates retrograding sequence
Prograding sequence

2 — Coarsening upward sequence having funnel shape indicates prograding sequence developed during sea level fall. This show catch up carbonates at shoreline

3 — Symmetrical trend indicates prograding (below) and retrograding (above)

4 — Cylindrical shape sequence shows aggrading sequence of keep-up carbonates at shallow water

5 — Coarsening upward sequence of funnel shape indicates prograding sequence in sea level fall

Fig. 20 Log response, depositional facies (electrofacies) and transgressive–regressive (T–R) sequences of the Lockhart Limestone in Meyal-10P
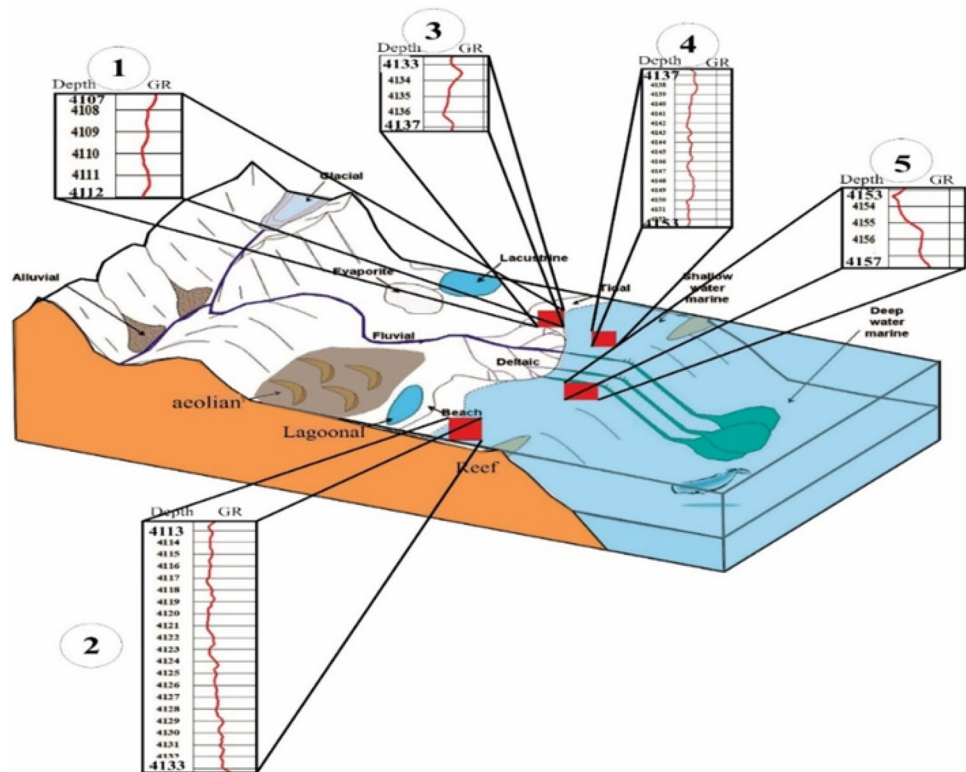
type of trend indicates the retrogradational sequence of the give-up carbonates at the tidal channel fill and tidal flat during the sea-level rise (Figs. 19, 21; Kendall 2003).

Bilal and Khan (2017) interpreted clastic-free shallow marine shelf conditions for the Lockhart Limestone. During the Upper Paleocene, the Lockhart Limestone containing benthonic foraminifera deposited during the transgression of the sea level (Bilal and Khan 2017).

Electrofacies 4 This is 15-m-thick (4137–4153 m) cylindrical shape interval which shows the aggradational sequence (Figs. 19, 21). The GR log values remain unchanged. Similarly, the resistivity log values also remain unchanged at the start but go toward the high value at the bottom (Figs. 19, 21; Kendall 2003).

The Lockhart Limestone is deposited in shallow to deep water of restricted inner shelf, near shore to inner shelf and inner to middle shelf environment of deposition due to the abundance of benthic foraminifera and lack of planktonic foraminifera (Khattak et al. 2017).

Electrofacies 5 This interval is 5-m-thick (4153–4158 m) with well-developed funnel shape indicating the progradational sequence (Figs. 19, 21). The GR values vary from low toward high, while the resistivity, density and SP log values remain unchanged. This type of trend indicates the depositional setting for the catch-up carbonates at the shore line (Kendall 2003). At this point, the sedimentary builds up change from clastics to carbonates during the sea-level rise (Figs. 19, 21; Kendall 2003).

According to Khan et al. (2016), the Lockhart Limestone represents a carbonate cyclic sequence marked by three, transgressive, deepening up cycles representing a gradual sea-level rise compensated by vertical accumulation of microfacies. The commencement of each cycle is clearly marked by the input of land-derived siliciclastic sediments and near shore-restricted marine faunal/floral assemblage in the inner shelf microfacies gradually thinning up section where the microfacies become deeper offshore (Khan et al. 2016). Overall the Lockhart Limestone is deposited in various sub-environments of marine environment varying from the tidal flat or tidal channel fill which has saline water influx through shallow water and shoreline which show deposition of catch-up carbonates (Figs. 19, 21; Kendall 2003).

Although the Lockhart Limestone is mainly composed of limestone, it has certain facies (electrofacies) on the basis of sea-level fluctuations. Sea-level fluctuations can easily be identified using GR log trends devised by Kendall (2003). The details of the depositional facies based on GR log (i.e., electrofacies) for the Lockhart Limestone in the Meyal-10P well are described as:

Electrofacies 1 This is ~ 5.4-m-thick (4118–4123.4 m) unit composed of three types of stacking patterns, i.e. starting from lower part, first the coarsening upward strata followed by fining upward sequence and again coarsening upward interval is present at the top (Figs. 20, 22). The GR log value, from the top of the interval, first increases, then decreases and then again increases in the lower most part;
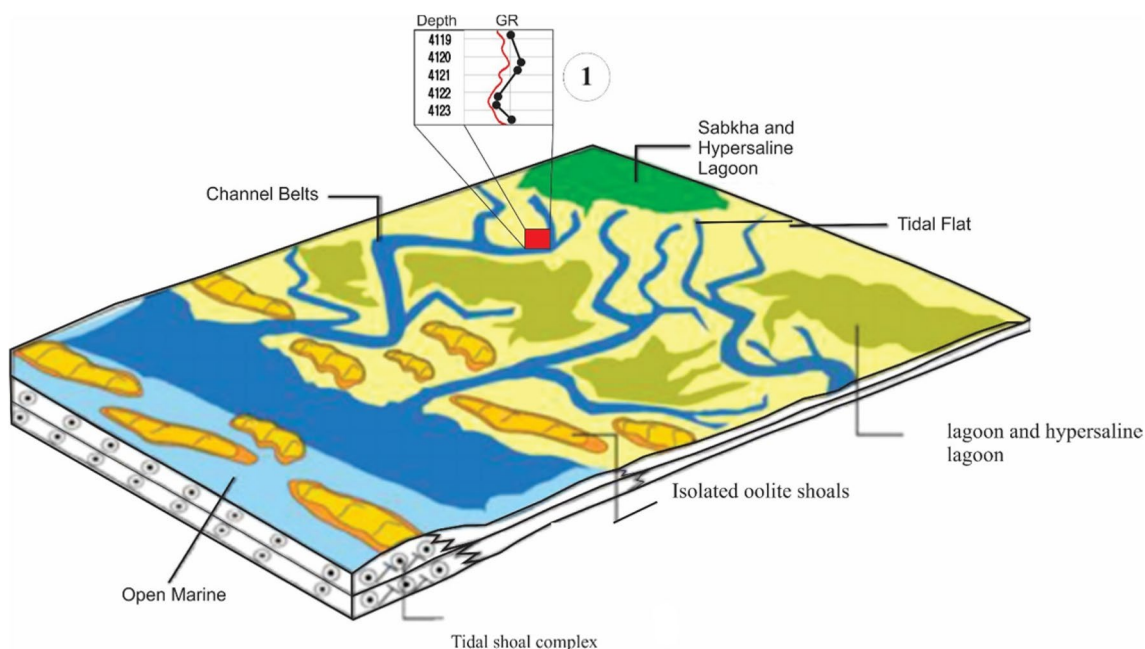
Fig. 22 Depositional model for electrofacies 1 of the Lockhart Limestone of Meyal-10P. The log trends are from GR log

same is the case with resistivity and density logs, while the SP log value remains unchanged. This trend indicates depositional settings of progradational stacking pattern in case of coarsening upward sequence and retrogradational sequence in terms of fining upward sequence (Figs. 20, 22; Kendall 2003).

In Kotal Pass Section of north Pakistan, inner to middle neritic shelf depositional system for Lockhart Limestone has been considered based on planktonic/benthonic ratio, the total foraminiferal abundance and their diversification (Afzal et al. 2005).

Electrofacies 2 This interval is 14-m-thick (4125–4139 m) having funnel shape (Figs. 20, 23). The GR and resistivity values for this interval increases downward, the density log values does not change, while the SP log value faces a minor variations from high value to low values. This trend indicates depositional setting of shore line, buildups, change from the clastics to carbonates (Kendall 2003). The carbonates deposited in this interval are called catch-up carbonates (Figs. 20, 23; Kendall 2003).

According to Khan et al. (2018), the Lockhart Limestone, exposed in Taxila, is interpreted to have been deposited in the fore-shoal mid-ramp, mid-ramp and outer ramp depositional environments. This limestone is characterized by siliciclastic wackestone microfacies thereby providing the evidence that the depositional settings were changed from clastics to the carbonates (Khan et al. 2018).

Electrofacies 3 This interval is 10-m-thick (4139–4149 m) almost symmetrical shape (Figs. 20, 23). The GR values for this interval first increase and then decrease; the resistivity values decrease and also SP curve bent toward low values, while the density log values remain unchanged. This trend shows a first rise in the sea level and then falls which indicates the depositional setting of carbonates at the offshore buildups, regressive-to-transgressive shore face (Figs. 20, 23; Kendall 2003). Sameeni et al. (2009) interpreted inner, middle and outer shelf environment of deposition for mudstone, wackestone and packstone microfacies of the Lockhart Limestone.

Electrofacies 4 This is 40-m-thick (4150–4190 m) interval of cylindrical shape (Figs. 20, 23). The GR log values for this interval are almost same marking a straight line showing no variation in the values. The SP log curve goes through a greater fluctuation from high value to lower value but the overall trend is from low to high values. The resistivity log shows sharp variation from high to low value. While the density log (RHOB) value remains the same, showing the carbonate lithology. This trend shows the aggrading stacking pattern of the depositional setting of heterogeneous facies in the shallow water (Figs. 20, 23; Kendall 2003). The Lockhart Limestone is entirely of shallow marine in origin with Paleocene biotic assemblages and minor shale (Yaseen et al. 2011).

Electrofacies 5 At the lower most part of the formation is ~ 3 m thick interval (4190 m to 4193 m) having the funnel shape coarsening upward sequence. The GR values shows variations from low to high. The resistivity log curve shows fluctuations, while the SP log values first increases and then decreases at the upper and lower parts of the interval-5
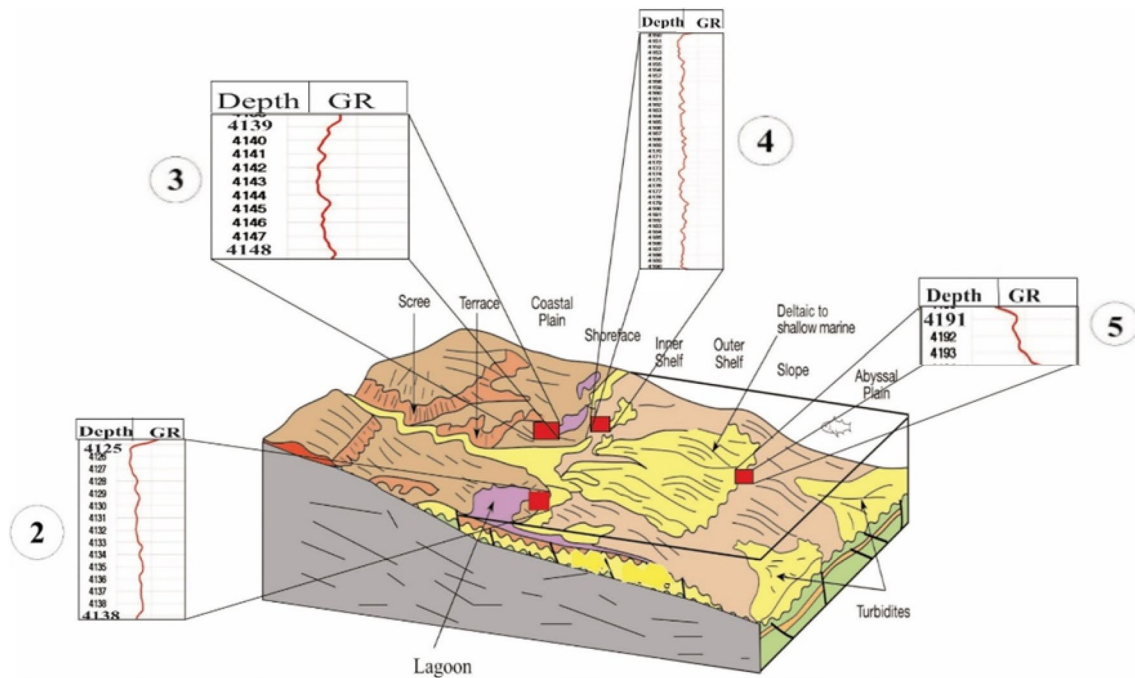
Fig. 23 Depositional model for Lockhart limestone of Meyal-10P. The log trends are from GR log

respectively. This trend indicates the depositional setting of carbonates at the shore line indicating the prograding stacking pattern (Figs. 20 and 23; Kendall 2003).

Conclusions

Petrophysical analysis, establishment of transgressive–regressive sequences and interpretation of depositional settings of the Lockhart Limestone, based on petrophysical logs, penetrated in two wells (Meyal-05P and Meyal-10P) of the Meyal Oil Field, Potwar sub-basin has been conducted. Based on the quantitative parameters, Lockhart Limestone of Meyal-10P is a good reservoir as compared to that of the Meyal-05P. In Meyal-05P and Meyal-10P wells, the average volume of shale is 48% and 20%; the range of density porosity is 1–5.6% and 1–31.7%; range of neutron porosity is 1–23% and 1–42.9%; the range of sonic porosity is 1–29% and 1–39%; the range of effective porosity is < 1–> 5% and 1–21%; and the range of hydrocarbon saturation is 92.21–99.8% and 97–99.6%. The Lockhart Limestone of Meyal-05P is a poor quality reservoir; however, the Lockhart Limestone of Meyal-10P well is a very good reservoir. In Lockhart Limestone of both wells, the permeability is < 0.1 mD. In Meyal-05P and Meyal-10P, the interpreted lithology of the Lockhart Limestone based on the petrophysical logs is predominated by limestone and minor shale (present in Meyal-10P only). The quantitative (very low permeability and very high hydrocarbon saturation) and qualitative

analysis reflects that the Lockhart Limestone is a tight reservoir. The Lockhart Limestone of both wells is deposited in different depositional environments showing the aggrading, prograding and retrograding depositional settings. The interpreted carbonate facies includes keep-up carbonates, catch-up carbonates and give-up carbonates implying fluctuations in the sea level.

References

Afzal J, Khan FR, Khan SN, Alam S, Jalal M (2005) Foraminiferal biostratigraphy and paleoenvironments of the Paleocene Lockhart Limestone from Kotal Pass, Kohat, Northern Pakistan. Pak J Hydrocarb Res 15:9–23

Ahmad S, Kroon D, Rigby S, Hanif M, Imraz M, Ahmad T, Jan IU, Ali A, Zahid M, Ali F (2014) Integrated paleoenvironmental, bio- and sequence-stratigraphic analysis of the late Thanetian Lockhart

Limestone in the Nammal Gorge section, western Salt Range, Pakistan. J Himal Earth Sci 47(1):9–24

Ahsan N, Shah MM (2017) Depositional setting and reservoir quality of the Lockhart Limestone (Lower Paleocene) in the Hazara-Kashmir Basin (NW Lesser Himalayas, Pakistan). AAPG datapages/search and discovery Article #90291. AAPG annual convention and exhibition, Houston, Texas, 2–5 April 2017

Ali TH, Ali F, Ali F, Haneef M, Hanif M, Ahmad S Jr, Rehman G, Fida S (2014) Microfacies analysis and diagenetic fabric of Lockhart Limestone exposed along Nathiagali-Murree road, district Abbottabad, Pakistan. J Himal Earth Sci 47(2):99–114

Anselmetti FS, Eberli GP (1997) Sonic velocity in carbonate sediments and rocks. In: Palaz I, Marfurt KJ (eds) Carbonate seismology, geophysical developments series, no. 6. Society of Exploration Geophysicists, Tulsa, pp 53–74

Armentrout JM, Malecek SJ, Fearn LB, Sheppard CE, Naylor PH, Miles AW, Desmariais RJ, Dunay RE (1993) Log-motif analysis of paleogene depositional system tracts, central and northern North Sea—defined by sequence stratigraphic analysis. In: Parker JR (ed) 4th Conference on the petroleum geology of northwest Europe, proceedings, no. 1. The Geological Society London, pp 45–57

Awais M, Ishaq M, Akhtar N (2012 and 2013) Geological mapping and structural analysis of a part of Kala-Chitta range, Kahi Village, Nizampur Khyber Pakhtunkhwa, Pakistan. J Hydrocarb Res 22, 23: 13–23

Bilal A, Khan MS (2017) Petrography of paleogene carbonates in Kalamula and Khursheedabad area, Kahuta, Azad Kashmir. Earth Sci Malays 1(1):36–41. https://doi.org/10.26480/esmy.01.2017.36.41

Bowen DW, Weimer P, Scarr AJ (1993) Application of siliciclastic sequence stratigraphy to exploration: examples from frontier and mature basins, SPE-26438, In: SPE annual technical conference and exhibition proceedings, v. omega, formation evaluation and reservoir geology: society of Petroleum Engineers, pp 221–233

Fertl WH, Vercellino WC (1978) Predict water cut from well logs. Practical log analysis, Part 4. Oil Gas J 76(25):111–116

Flügel E (2010) Microfacies analysis of Limestone. Springer, Berlin

Ghazi S, Aziz T, Khalid P, Sahraeyan M (2014) Petroleum play analysis of the Jurassic sequence, Meyal-field, Potwar basin, Pakistan. J Geol Soc India 84:727. https://doi.org/10.1007/s12594-014-0183-2

Ghorab M, Ramadan AM, Nouh AZ (2008) The relation between shale origin (source or non source) and its type for Abu Roash formation at Wadi-El Naturn area, south of Western Desert, Egypt. Aust J Basic Appl Sci 2(3):360–371

Hanif M, Imraz M, Ali F, Haneef M, Saboor A, Iqbal S, Ahmad S Jr (2013) The inner ramp facies of the Thanetian Lockhart formation, western Salt Range, Indus Basin, Pakistan. Arab J Geosci 7(11):4911–4926

Hasany ST, Saleem U (2012) An integrated subsurface geological and engineering study of Meyal Field, Potwar Plateau, Pakistan. American Association of Petroleum Geologists, Search and Discovery Article # 20151

Kadri IB (1995) Petroleum geology of Pakistan. Pakistan Petroleum Limited, Karachi

Kazmi AH, Jan MQ (1997) Geology and tectonics of Pakistan. Graphic Publishers, Karachi

Kazmi AH, Rana RA (1982) Tectonic map of Pakistan, scale 1:2000000, 1st edn. Geological Survey of Pakistan, Quetta

Kendall C (2003) Use of well logs for sequence stratigraphic interpretation of the subsurface. USC Sequence Stratigraphy Web. University of South Carolina. http://www.sepmstrata.org/page.aspx?&pageid=35&6

Khan MW, Alam I, Shah MZ (2016) Microfacies and diagenetic fabric of the Lockhart Limestone, Kotal Pass section, northeast of Kohat, Pakistan. Int J Econ Environ Geol 7(1):64–72

Khan M, Khan MA, Shami BA, Awais A (2018) Microfacies analysis and diagenetic fabric of the Lockhart Limestone exposed near Taxila, Margalla Hill Range, Punjab, Pakistan. Arab J Geosci. https://doi.org/10.1007/s12517-017-3367-4

Khattak Z, Khan MA, Rahman Z, Ishfaque M, Yasin M (2017) Microfacies and diagenetic analysis of Lockhart Limestone, Shah Alla Ditta area Islamabad, Pakistan. Pak J Geol 1(1):24–26. https://doi.org/10.26480/pjg.01.2017.24.26

Lucia FJ (2007) Carbonate reservoir characterization, an integrated approach, 2nd edn. Springer, Berlin

Malik AM, Ahmed N (2014) Paleocene carbonate of Kohat-Potwar sub-basin of Upper Indus Basin, Pakistan. Sci Int (Lahore) 26(5):2337–2350

Nawaz M, Nisar UB, Bukhari SAA, Khan S (2015) Petrophysical analysis of Lockhart Limestone with porosity and thickness correlation of exposed Lockhart Limestone at Nathia Gali with subsurface Lockhart Limestone of Chanda deep-01 well in Upper Indus basin. J Himal Earth Sci 48(1):59–63

Rider M (1996) The geological interpretation of well logs, 2nd edn. Whittles Publishing, Scotland

Saddique B, Ali N, Jan IU, Hanif M, Shah SA, Saleem I, Faizi MM, Arafat MY (2016) Petrophysical analysis of the reservoir intervals in Kahi-01 well, Kohat Sub-Basin, Pakistan. J Himal Earth Sci 49(1):30–40

Sameeni SJ, Nazir N, Abdul-Karim A (2009) Foraminiferal biostratigraphy and reconnaissance microfacies of Paleocene Lockhart Limestone of Jabri area, Hazara, northern Pakistan. Geol Bull Punjab Univ 44:85–96

Sameeni SJ, Haneef M, Shabbir F, Ahsan N, Ahmad N (2013) Biostratigraphic studies of Lockhart Limestone, Changlagali area, Nathiagali-Murree road, Hazara, northern Pakistan. Sci Int (Lahore) 25(3):543–550

Schlumberger (2009) Log interpretation charts. 225 Schlumberger Drive, Sugar Land, Texas 77478, p 50

Serra O (1985) Sedimentary environments from wireline logs. Schlumberger, Houston

Shah SMI (2009) Stratigraphy of Pakistan. Memoirs of the Geological Survey of Pakistan 22, pp 243–244

Siyar SM, Awais M, Zafar M, Waqas M, Faisal S (2018) Reservoir characterization of Paleocene clastics and carbonates in Chanda-01 well, Kohat Basin, Khyber Pakhtunkhwa, Pakistan: a petrophysical approach. Nucleus 55(1):27–32

Vail PR, Wornardt WW (1990) Well log-seismic sequence stratigraphy: an intergrated tool for the 90'S. GCSSEPM foundation eleventh annual research conference

Wagoner JCV, Mttchum RM, Campion KM, Rahmanian VD (1990) Siliciclastic sequence stratigraphy in well logs, cores and outcrop: concepts for high resolution correlation of time and facies. American Association of Petroleum Geologists, Methods in Exploration Series 7

Yaseen A, Rajpar AR, Munir M, Roohi G, Rehman KU (2011) Micropaleontology of Lockhart Limestone (Paleocene), Nilawahan Gorge, Central Salt Range, Pakistan. J Himal Earth Sci 44(2):9–16